Available online at www.sciencedirect.com
ScienceDirect
Polymer 48 (2007) 5098–5106
polymer
www.elsevier.com/locate/polymer

Influence of molecular architecture and melt rheological characteristic on the optical properties of LDPE blown films

Haijin Zhu [a,c], Yanfang Wang [b], Xiuqin Zhang [a,c], Yifan Su [b], Xia Dong [a], Qingkui Chen [b], Ying Zhao [a], Cun Geng [b], Shannong Zhu [a], Charles C. Han [a], Dujin Wang [a,*]

[a] *Beijing National Laboratory for Molecular Sciences, CAS Key Laboratory of Engineering Plastics, Joint Laboratory of Polymer Science and Materials, Institute of Chemistry, The Chinese Academy of Sciences, Beijing 100080, China*
[b] *Resin Applications Research Institute, Sinopec Beijing Yanshan Petrochemical Group Co., Ltd, Beijing 102500, China*
[c] *Graduate School of the Chinese Academy of Sciences, Beijing 100080, China*

Received 18 April 2007; received in revised form 19 June 2007; accepted 21 June 2007
Available online 26 June 2007

Abstract

A systematic investigation on the origin of the haze of LDPE blown films was conducted, aiming to correlate the film haze with the molecular architecture and melt rheological properties. First of all, the haze measurement indicated that the surface haze, rather than the bulk haze, is the dominating factor for the total haze of the investigated films. No spherulitic crystals or other superstructures were observed for the LDPE blown films, implying that the crystallites formed in the film-blowing process are too small to be responsible for the optical haze. Rheological study revealed that the surface roughness was originated from the irregular flow of LDPE melt during the extrusion process. NMR, GPC and parallel-plate rheology were applied to study the molecular architecture of the LDPE resins. It was found that the LDPE sample with higher haze value exhibits distinctly larger portion of higher molecular weight component, broader molar mass distribution, significantly higher side chain branch density.

Keywords: Low-density polyethylene (LDPE); Haze; Rheology

1. Introduction

The optical property of blown LDPE films, including haze, transparency or clarity, gloss and transmittance is critical to end use. The haze of a film is defined as the fraction of (normal incident) transmitted light that deviates from the directly transmitted beam by more than 2.5° [1]. For blown LDPE films, haze may originate from light scattering caused by both bulk inhomogeneities and surface roughness [2]. It was recognized in the early time that haze was caused primarily by the light scattering due to surface irregularities [3–6]. Early experimental literature on the haze of PE blown films was reviewed by Willmouth [1]. According to early literatures, two main reasons account for the surface roughness: flow-induced irregularities and protruding crystalline structures. The former is a well-known rheological effect which can be ultimately correlated with molecular architecture. Crystallization roughness was postulated to occur due to the formation of crystalline aggregates on or close to the surface of the films [7].

From the experimental viewpoint, later studies have confirmed that flow defects and crystalline structure induced surface roughness is the major source of the haze of blown films. White et al. studied a wide range of semi-crystalline (LDPE, HDPE, LLDPE, PP and PBT) and amorphous (PS and PMMA) materials, and found that the crystallization is the primary reason for the surface roughness, while the rheological effect played a secondary but important role [7]. For conventional LDPE blown films, melt elasticity is the main cause of

* Corresponding author.
E-mail address: djwang@iccas.ac.cn (D. Wang).

0032-3861/$ - see front matter © 2007 Elsevier Ltd. All rights reserved.
doi:10.1016/j.polymer.2007.06.044

haze, while the high haze of HDPE is usually attributed to the high crystallization degree [8]. Several authors have studied the relationship between micrometer-scale structure and turbidity in blown films [6,9–11]. Hashimoto and co-workers reported the formation of sheaf-like superstructures on the surface of tubular extruded polybutene films [12]. They concluded that the sheaf-like structures causes light to scatter from the surface of the films. Pinto and Larena studied the optical properties of polyethylene tubular films [13]. The results showed that light scattering is strongly correlated with the surface roughness, and the crystallinity in the bulk plays a secondary role.

From the theoretical point of view, the degree of light scattering depends on the size of the scattering unit, typically the crystalline structure presented on the surface or in the bulk of the film for semi-crystalline polymer. If such structures are of the wavelength scale of visible light, considerable diffuse reflection, refraction, and scattering will occur, resulting in turbidity. Therefore, the size of these scattering units plays a key role in deciding the optical property of the films. There are numerous studies on visible light scattered by bulk inhomogeneities and/or rough surfaces [1,14]. Haze has been calculated as function of bulk inhomogeneities [1], but theoretical study on the relationship of haze and surface roughness is sparse. Wang et al. proposed a method for haze calculation [15]. Based on the approximation that the surfaces were spherulitic, the combined scattering of the surfaces could be modeled by Mie scattering theory which is valid for a single sphere or any size and refractive index. The calculated results agree well with experimental data for films of six different materials. According to the model, haze will reach a maximum value at the spherulite diameter of 800 nm (incident beam $\lambda = 550$ nm). Although this model provides insight into the relationship between surface roughness and haze, it cannot account for non-spherical case which is more common.

Most of the previous research concentrated on the relationship between the structures and the haze of the films. In the present paper, however, we have made one step further through the investigation of the influence of the macromolecular chain architecture, crystallization structure, grain size, surface morphology as well as the rheological behavior on the optical properties including haze. The three LDPE films reported in this article have completely the same processing conditions and almost the same transparency (see Table 1), but show remarkably different haze. The main aim of this work is to establish the relationship between the optical properties and the molecular architecture parameters, further to gain some insight into the key parameters controlling the optical performance of LDPE blown films.

2. Experimental

2.1. Materials

The three commercial low-density polyethylene blown-film samples used in this study were supplied by Sinopec Beijing Yanshan Petrochemical Corporation. Sample resins LD1 and LD2 were produced with tubular technique, and sample resin LD3 was produced with autoclave technique. Table 1 shows the characterization data of the three resins provided by the manufacturer.

The three corresponding blown films to be tested were produced by an Alpha blown film machine group. A screw extruder with diameter of 45 mm and *L/D* of 28 was used, and the diameter of the die was 100 mm. The die gap was 0.84 mm. All the films were made with a constant drawing rate of 17.6 m/min, and the thicknesses were 30 μm, 30 μm and 35 μm for LD1, LD2 and LD3, respectively.

2.2. Haze measurements

A Toyo Seiki Seisakusho Ltd. No. 206 direct reading haze meter was used for haze measurements according to ASTM D 1003-97. The percentage of light scattered more than 2.5° when penetrating a film sample was measured and the values used in this study are averages of five measurements. Light scattering on the surface as well as in the bulk contributes to the haze value. Bulk contribution was estimated by measuring haze of films covered with polymethylphenyl siloxane fluid (silicon oil) on both sides, and the difference between total haze and bulk haze gave surface haze. The silicon oil has a refractive index of 1.51, which is almost the same as that of the polyethylene blown films (1.50–1.52). The silicon oil was kindly donated by Zhong Lan Chen Guang Chemical Engineering Academy in Sichuan Province, P.R. China.

2.3. Differential scanning calorimetric (DSC) analysis

DSC measurements were performed on a Perkin–Elmer DSC-7 apparatus at a heating rate of 10 °C/min. About 4 mg of the film sample was cut into small pieces and sealed in an aluminum pan. The calibration of the temperature scale and the heat flow was achieved from the melting scans of high-purity indium and zinc samples at the same heating rate. The melting point of the materials was determined at the peak of the endotherms of the first heating scan. Crystallinity was calculated by Eq. (1):

Table 1
Parameters of commercial LDPE resin and film samples

Samples	Density/(g/cm^3)	MI (190 °C/2.16 kg)/(g/10 min)	Branch content[a]/(CH_3/1000C)	Transparency/%	Haze/%
LD1	0.925	2.08	14.8	91.0	6.2
LD2	0.923	1.99	22	91.2	7.9
LD3	0.919	1.55	21.5	90.1	26.8

[a] Total number of short and long branches obtained from FTIR spectroscopy [16].

$$X_c = \frac{\Delta H_u}{\Delta H_{100}} \times 100\% \quad (1)$$

where ΔH_u is the integrated melting enthalpy between 0 °C and 140 °C from the DSC endothermic curve and ΔH_{100} is the melting enthalpy of polyethylene crystal with 100% crystallinity, which is set as 290 J/g in this study [17]. The lamellar thickness l_c can be calculated by Thomson–Gibbs equation:

$$T_m = T_m^0(1 - 2\delta_e/(\Delta H \cdot l_c)) \quad (2)$$

where T_m^0 is the equilibrium melting point of an infinitely thick polyethylene crystal, δ_e the surface energy of a polyethylene crystal, and ΔH the enthalpy of fusion per unit volume. Here, the values of $T_m^0 = 415$ K, $\delta_e = 93$ mJ/m^2 and $\Delta H = 300$ J/cm^3 for polyethylene were recommended by Kuwabara et al. [18].

2.4. Nuclear magnetic resonance (NMR) spectroscopy

^{13}C NMR measurements were carried out at 120 °C on a Bruker DRX400 NMR spectrometer at a resonance frequency of 100.62 MHz. LDPE/*o*-dichlorobenzene solutions (15 wt%) were prepared with 1 wt% TMS (tetra methyl silane) as internal chemical shift reference. The peak assignments of different carbon atoms along the molecular chain adopted for the absorption bands in NMR spectra and the calculation of branch contents were carried out according to Zhu [19].

2.5. Gel permeation chromatography (GPC)

The molecular weight (MW) and molecular weight distribution (MWD) were determined by using a Waters Alliance GPCV 2000 equipped with differential refractive index detector. 1,2,4-Trichlorobenzene was used as the elution solvent. The operating temperature was 160 °C, and mono-dispersed polystyrene standards were used for making the calibration curve.

2.6. Wide angle X-ray diffraction (WAXD)

WAXD measurements were conducted on a Rigaku D/Max-2500 powder X-ray diffractometer using Cu Kα radiation (40 kV, 200 mA). The X-ray wavelength used was 0.154 nm; 0.02° step and 2θ range of 4–40° were selected. The average sizes perpendicular to the crystal panel can be calculated by full-width half-maximum value. The measurements and calculations were done by MDI Jade 5.0 (SP1) software automatically.

2.7. Scanning electron microscope (SEM)

The LDPE blown films were coated with Au and then studied by a Hitachi S-2150 scanning electron microscope, fitted with a field emission source and operating at an accelerating voltage of 25 kV.

2.8. Rheology

Stress relaxation test, steady rate sweep test and dynamic frequency sweep test were performed on a strain-controlled ARES (TA) rheometer with a pair of parallel-plate configuration. The LDPE resins were hot-pressed into a pellet with diameter of 25 mm and thickness of ca. 1 mm for measurements. All tests were performed under a dry nitrogen atmosphere. Dynamic strain sweep tests were always conducted before dynamic frequency sweep tests to ascertain the linearity of the viscoelastic regime. Strain of 5% was selected for the dynamic frequency sweep experiment of all the three samples. The measurement temperature is 190 °C, except the cases where activation energy of flow is required, where the range is 150–190 °C, using a new sample at each temperature. Zero-shear viscosity η^0 is estimated using the Vinogradov–Malkin equation fit of dynamic complex viscosity η^* *vs* radian frequency.

The capillary rheology experiments were performed on a Rosand RH7 Advanced Capillary Rheometer (Bohlin Company, Britain). The diameter of the die is 2 mm, and the *L/D* of the capillary is 16; the experiment was carried out at 190 °C. About 4 cm of the extruded specimen was cut for measurement. Average of five measurements was used in the analysis.

3. Results and discussion

3.1. Relationship between haze and microstructure in LDPE films

Haze of blown polymer films has been generally thought to be caused by both surface irregularities and heterogeneity of bulk density. Islands of crystal domains in the amorphous ocean were thought to be mainly account for higher haze [2,8,20], however, this viewpoint is untenable in the case of LDPE blown films based on our experiments. The DSC exothermic curves for LDPE films are presented in Fig. 1. The detailed parameters of DSC measurements are given in Table 2.

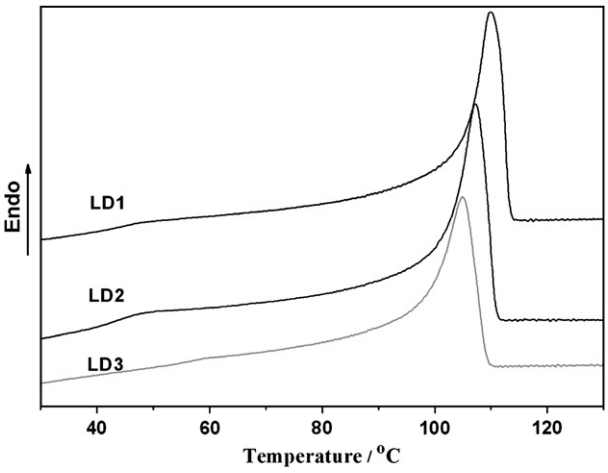

Fig. 1. Melting endothermic curves of LDPE blown films. The haze decreases from top to bottom.

Table 2
Detailed thermal and crystalline behaviors of LDPE blown films

Sample	T_m[a]/°C	ΔH_c/(J/g)	X_c/%	l_c/nm
LD1	109.8	97.8	33.7	8.0
LD2	107.2	91.6	31.6	7.4
LD3	104.9	83.4	28.8	6.9

[a] The primary peak temperature on DSC endotherms was taken as the melting point.

LD1 showed the highest T_m and ΔH_c, whereas LD3 had the lowest. The total haze increases with the decrease of melting temperature and crystallinity (See Tables 1 and 2), so it can be concluded that the haze of LDPE blown films is not affected by the bulk crystallization behavior directly, since haze is generally considered to be adversely affected by crystallinity. This is likely to be attributed to the fact that the size of the scattering units in the bulk is much smaller than the averaged wavelength of visible light. The lamellar thickness is related to the melting temperature, and it can be determined by using Thomson–Gibbs equation. As can be seen in Table 2, the lamellar thickness, ranging from 5 to 10 nm, is much smaller than the wavelength of visible light, typically in the range of 400–700 nm. Therefore, it can be concluded that the lamellar crystallite is not an effective unit to cause light scattering. Moreover, lamellar thickness deduced from DSC experiments can give quantitative information about side chain branching content of the LDPE molecules, which can be compared with NMR results (shown later on). The bulk haze might be attributed to the crystals consisting of well-organized lamellar structure or the aggregates of crystals. In order to clearly illustrate the crystallite size in the bulk of the blown films, untreated blown films were directly subjected to WAXD measurement. The diffraction curves in Fig. 2 obviously show that sample LD1 has the highest crystallinity, whereas sample LD3 has the smallest. This result is apparently consistent with the crystallinity of the three LDPE blown films

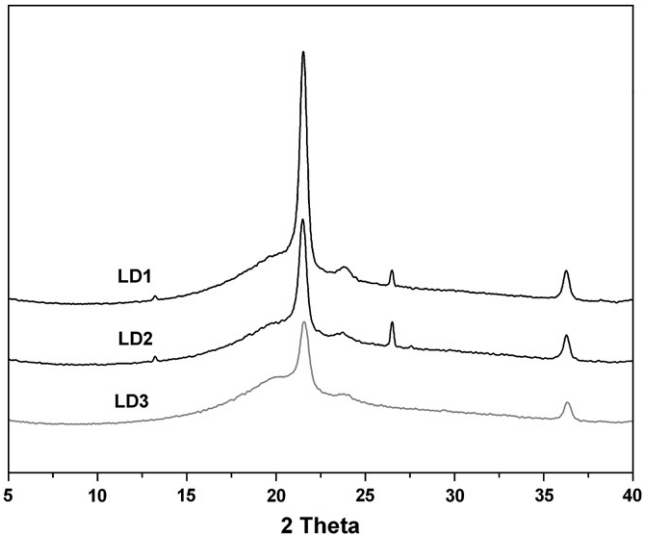

Fig. 2. WAXD curves of LDPE blown films. The haze decreases from top to bottom.

Table 3
Crystallite sizes of the LDPE blown films

Crystal planes	LD1/nm	LD2/nm	LD3/nm
110	17.9	17.3	14.9
200	13.4	13.1	13.5

investigated by DSC (Fig. 1), though the absolute value varies a little. The crystallite sizes of the films are listed in Table 3. It is noted that the crystallite size of 200 planes of the three films is almost the same, with that of 110 plane of LD3 is remarkable smaller than those of LD1 and LD2. It is also noteworthy that the crystallite sizes in the LDPE films are a little bit larger than the lamellar thickness, yet still smaller than the wavelength of visible light, meaning that the crystallites in the bulk film cannot account for the haze of the LDPE blown films.

To elucidate the origin of the film haze, the total, surface and bulk haze were measured (see Table 4). The percentage of the surface haze conclusively shows that the vast majority of the total haze of these LDPE blown films comes from the surface roughness contribution. In addition, the observed bulk haze of the LDPE blown films does not show much difference. It is believed that the observed bulk haze may not necessarily originate from the bulk, but from the mismatching of refraction index of LDPE and silicon oil, as well as the tiny air bubbles and some other impurities existing on the surface. So, basically the bulk haze is neglectable. Little haze contribution from the bulk may be due to the very small bulk crystallites, which will not cause effective light scattering.

From the SEM micrographs (Fig. 3), it is observed that all the blown films show tuber morphology, and the fine texture of these tubers is different for the three sample films. The superficial up-and-down structure of LD1 and LD2 is quite similar, though that of LD3 is much more fluctuant at micrometer scale. The result of SEM accords well with the haze value listed in Table 4.

The above combined investigation on the microscopic structures of different LDPE blown films can unequivocally give a conclusion that the haze of the LDPE blown films arises mainly from surface irregularities. The surface roughness can be affected by the melt elasticity both via nucleation and flow instabilities. Hence, the focused issue is what type of surface irregularities existed on the blown LDPE films that cause the majority of surface haze – the rheological instabilities, the crystal textures on the surface of the films or any other factors? To address this point, both capillary and parallel-plate rheological measurements were carried out to study the LDPE melt properties.

Table 4
Haze measurements of LDPE blown films

Samples	Haze			Percentage of surface haze/%
	Total	Bulk	Surface	
LD1	6.2	0.9	5.3	85.5
LD2	7.9	1.1	6.8	86.1
LD3	26.8	0.8	26	97.0

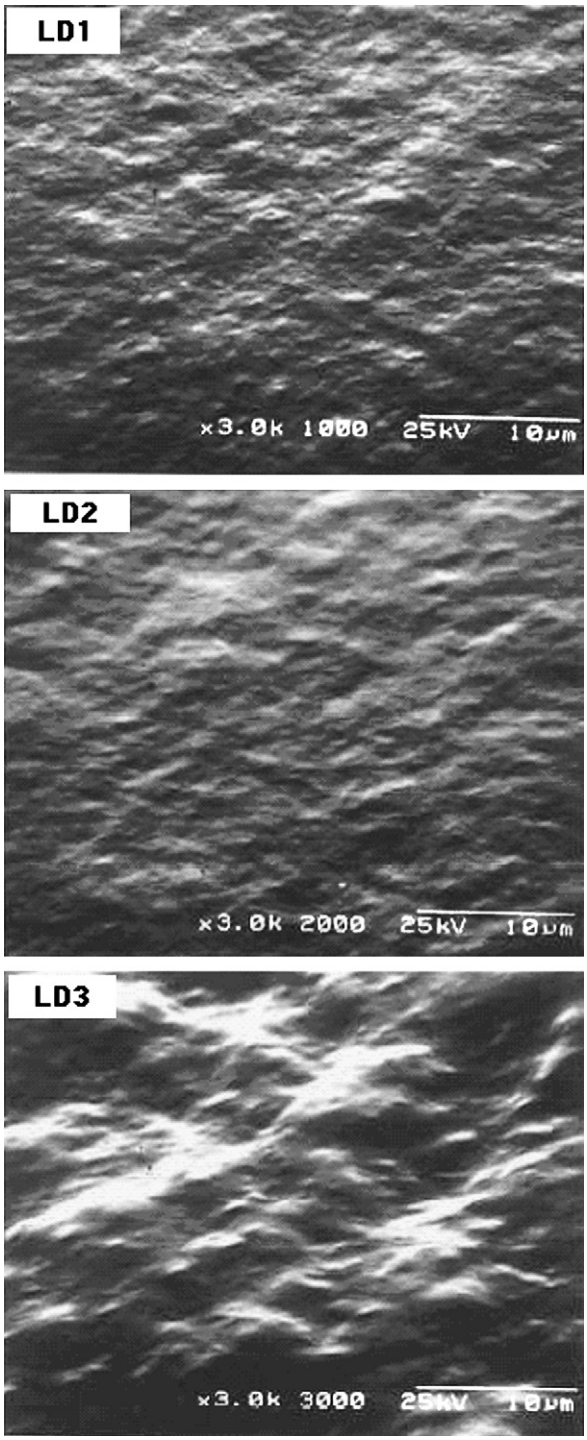

Fig. 3. SEM micrographs of LDPE blown films.

The plot of die swell ratio *vs* shear rate is shown in Fig. 4, which clearly indicates that sample LD3 displays much higher die swell ratio than the other two samples, while sample LD1 shows the lowest die swell ratio and LD2 the medium. It should also be noted that the die swell ratio curve of sample LD3 terminates at a very low shear rate because of melt fracture, implying instability of the LDPE melt. The surface distortions of the necessary scale in the relevant stress range are also observed for all of the three samples. The hazes of

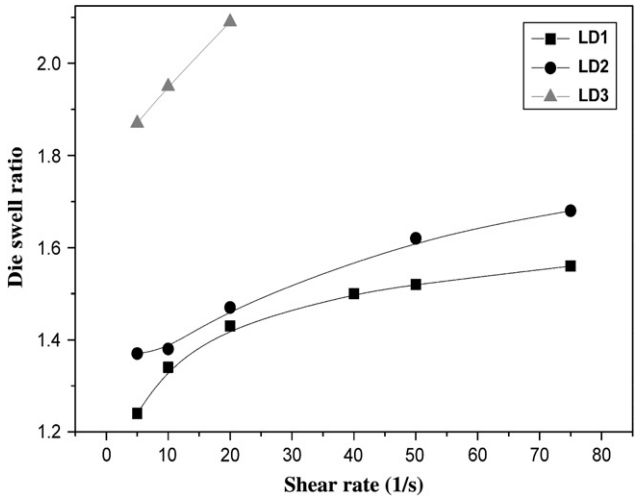

Fig. 4. Plot of die swell ratio *vs* shear rate for LDPE melts.

these LDPE blown films may originate from the instability of the melt flow near the die exit, thus causing severe surface irregularities. This conclusion is strongly supported by the transient rheological data presented in Fig. 5. Apparently, sample LD3 shows significantly lower stress at the very beginning of the experiment, whereas LD1 shows slightly higher stress than LD2. Moreover, the melt stress of LD3 decays with a slower rate than the other two samples, meaning that sample LD3 has the longer relaxation time at a given shear strain, whereas that of LD1 shows the fastest decaying rate, i.e., shortest relaxation time. The polymer melt outside of the die is able to relax adequately before temperature goes down to the freezing point, so the surface inhomogeneity originated from extrusion instability or other reasons can be alleviated by the smoothing effect of the film tension. As for sample LD3, it is believed that localized melt fracture occurred because of the high shear viscosity and the relatively high shear rate on the outer layer of the melt close to the die, and the surface roughness cannot be alleviated efficiently before the melt was quenched by air because of its slow relaxation. In

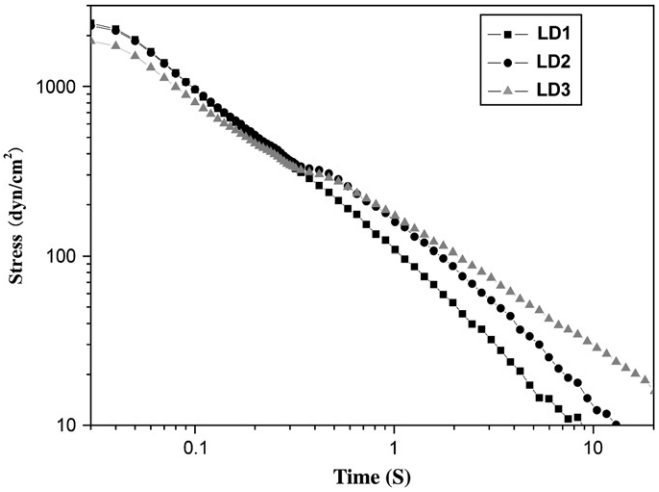

Fig. 5. Plot of log t *vs* τ for LDPE melts.

addition, slow relaxation rate can also prevent the macromolecules from arranging into regular or perfect spherulitic crystals, so there will be no spherulitic crystals or other superstructures present. Therefore, vast majority of the haze of sample LD3 comes forth before the melt undergoes crystallization, although there is still some contribution from later crystallization effect. The former conclusion can be validated by the results of polarized optical microscopy and small angle laser light scattering experiments. Neither Maltese cross which is characteristic of spherulitic crystals was observed in the POM images nor did the characteristic 'four leaf clover' pattern for spherulitic crystals present in the SALLS patterns. Sukhadia et al. studied the blown-film haze of a large types of PE resins and divided the haze varieties into three regimes according to the causative mechanisms, i.e., crystallization haze regime, intermediate haze regime and extrusion haze regime [21]. PE resins lying in the intermediate regime generally show the lowest haze value, so samples LD1 and LD2 should be classified in the intermediate regime, as no sign of spherulitic structure or some other superstructures was observed and the samples show relatively low melt elasticity and short relaxation time. Sample LD3, however, lies in the extrusion haze regime according to Sukhadia's classification.

3.2. Correlation between haze and molecular architectures in LDPE

From the above discussion, it is concluded that the surface irregularities which lie in the wavelength scale of visible light (400–700 nm) account for vast majority of the haze of LDPE blown films. The haze of the three LDPE blown films studied has been confirmed to depend on the rheological properties of the melts rather than the crystallinity or crystallization behaviors. Hence, the focused issue is: how does the molecular architecture affect the surface roughness of LDPE blown films through rheological behavior? To address this key point, we performed the experimental investigations including nuclear magnetic resonance spectroscopy, gel permeation chromatography and parallel-plate rheology; all of which have been well proved to be effective tools in characterizing molecular structures of polymers.

Table 5 shows the averaged molecular weights and corresponding polydispersity indices of the three LDPE resins determined by GPC. Obviously, although the samples have similar number average molar masses (M_n), they are characterized by distinct weight average molar masses, and therefore, different molar mass distributions. The weight average molar mass for sample LD3 is remarkably higher than the other

Table 5
Molecular weight and distribution characterization of three LDPE samples

	LD1	LD2	LD3
M_n[a]	1.65×10^4	1.72×10^4	1.30×10^4
M_w[a]	1.50×10^5	1.65×10^5	4.11×10^5
Polydispersity index	9.10	9.59	31.5

[a] Number and weight average molar masses in daltons.

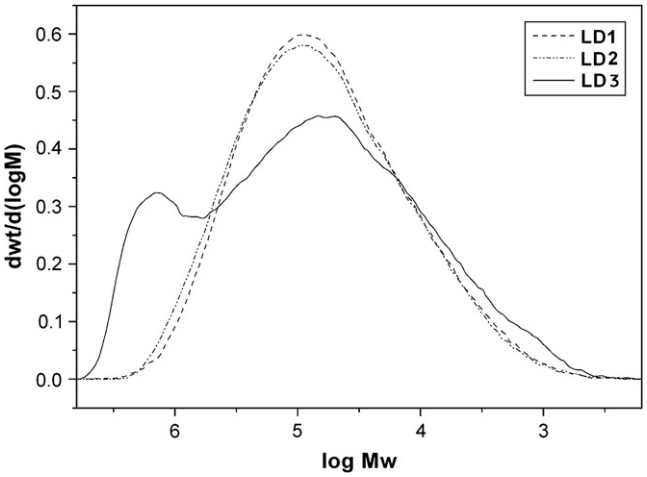

Fig. 6. Apparent molecular weight and molecular weight distribution curves for LDPE resins.

two samples. The apparent molecular weight and molecular weight distribution curves for the three LDPE resins are shown in Fig. 6. These curves are referred to as apparent molecular weight distribution, since the data are not corrected in the presence of long-chain branching.

As indicated in Fig. 6, sample LD3 which has significantly higher haze holds significantly much higher molecular weight species than the other two samples, indicating a large population of large, highly long-chain branched LDPE molecules. It is also interesting to notice that, differing from the other two resins, sample LD3 shows apparent bimodal molecular weight distribution. Sample LD2 appears to have a broader molecular weight distribution and slightly larger portion of high molecular weight molecules than sample LD1. The small amount of very high molecular weight polymer is thought to be the key factor in determining melt elasticity, and consequently affecting the film's optical properties. It is well known that shear modification is widely used in industry to enhance LDPE blown film's optical properties [22–24], the purpose of which is to scissor the big molecules into smaller ones and thus narrowing the molar mass distribution. Therefore, it is understandable that, due to existence of the relatively high molecular weight moieties in sample LD3, the melt elasticity of the corresponding melt is much higher than the other LDPE samples, leading to the low flow stability in the film-blowing process.

The characterization of branching in LDPE resins is crucial to the comprehension of their melt processing behavior. The side chain branching content has been evaluated by ^{13}C NMR spectroscopy in this work. It must be kept in mind that the NMR approach cannot distinguish between branch lengths equal to or longer than six carbon atoms, and it is also helpless for discerning branching levels below about $1/10^4$ carbon atoms. The side chain branching values are presented in Table 6. It is clear that samples with higher haze value generally have much larger side-chain groups, as well as the overall branch density. The side chain branch density can also be obtained from the melting temperature determined

Table 6
Side chain branching values of the three LDPE resins determined by NMR[a]

Sample	Content of various branches in 10,000C				Branch density/10,000C
	Methyl	Ethyl	Butyl	Hexyl[b]	
LD1	Rare	33	40	53	126
LD2	40	14	45	61	160
LD3	0	29	62	80	171

[a] The calculation was based on two assumptions: (1) Nuclear Overhauser enhancement effect arising from proton decoupling is averaged in macromolecules; (2) Waiting time of 5 s used in the experiments is long enough for the relaxation of all the carbon atoms in the polymer chain.
[b] Including side branches longer than six carbons.

by DSC. The average methylene sequence length (ASL) can be obtained from DSC endotherms, where the melting temperature was transformed into ASL by using a calibration generated from standard hydrocarbons. The calibration between the composition and the melting temperature had been done by Keating et al. [25].

$$\ln(X) = 0.331 - 135.5/T_m \quad (3)$$

where X represents the mole fraction of carbon in CH_2 groups in the linear hydrocarbon, e.g., $X = 0.900$ for n-$C_{20}H_{42}$, and T_m is the melting temperature in kelvin (peak of the endotherm). It should be pointed out that the crystallization of branching polyethylene may differ from that of linear molecules used as a model in the Keating method. However, in the absence of better standard samples, the use of linear paraffin as a model appears to provide reasonable results in many cases [26]. The branch density (BD) per 10,000 carbons can be calculated by the following equation:

$$BD_{DSC} = 10,000(1 - X)/2 \quad (4)$$

The BD values calculated by melting temperature are compared with that originated from NMR spectra (Table 7). The results from the two methods show well agreement with each other, although the values calculated from DSC endotherms are systematically lower than those from NMR spectra. However, it is reasonable when considering the fact that the BD_{DSC} represents the branch density of crystalline part, whereas BD_{NMR} represents the branch density of overall polymer including crystalline part and non-crystalline part. It is generally accepted that the methylene segments of polyethylene molecules with less side branches prefer to enter crystal lattice, while those with more and larger side chains are more prone to stay in the amorphous region. Therefore, the BD in crystalline domains will be lower than in the amorphous region, and certainly lower than the overall branch density.

Table 7
Branch density values determined by NMR and DSC

Branch density	LD1	LD2	LD3
BD_{NMR}[a]/10,000C	125	160	171
BD_{DSC}[a]/10,000C	113	124	135

[a] BD_{NMR} represents the branch density determined by NMR; BD_{DSC} by DSC.

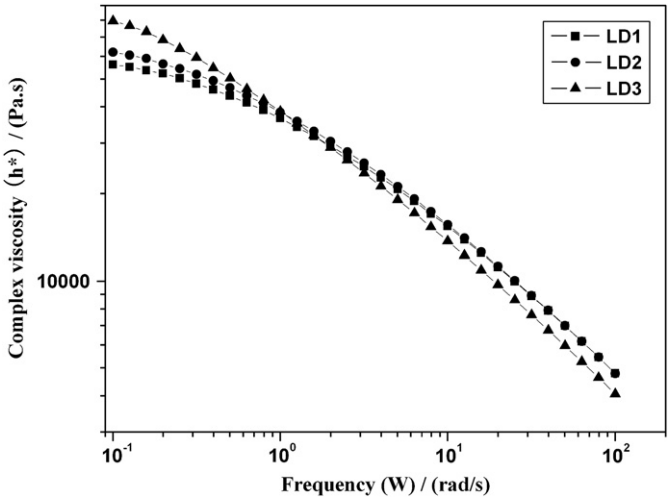

Fig. 7. Plot of log η^* *vs* log ω for the LDPE melts.

The melt property of LDPE depends strongly on the molecular weight, molecular weight distribution, branch density, length of side chains, and so forth. Especially, long-chain branches play a decisive role in affecting melt elasticity, which can be sensitively detected by rheological method. Dynamic frequency sweep test (Fig. 7) and steady rate sweep test (Fig. 8) were performed to study the relationship between the molecular architecture and the rheological behavior. It is observed in Fig. 7 that at low frequency sample LD3 shows the highest viscosity, whereas sample LD1 the lowest. The different rheological behaviors in the shear viscosity at very low frequency can be explained by molecular weight: high viscosity at low frequency usually indicates high molecular weight. Again, the shear thinning trend of LD3 is much faster than the other two samples as indicated in both Figs. 7 and 8. This is likely to be attributed to the broad molecular weight distribution of LD3. It is commonly recognized that small amount of LCB have pronounced effects on the melt flow behavior [27].

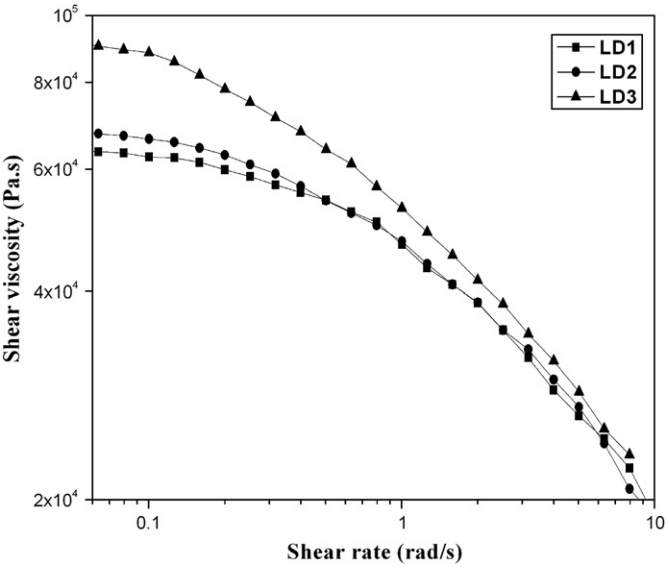

Fig. 8. Plot of shear viscosity (η) *vs* log γ for the LDPE melts.

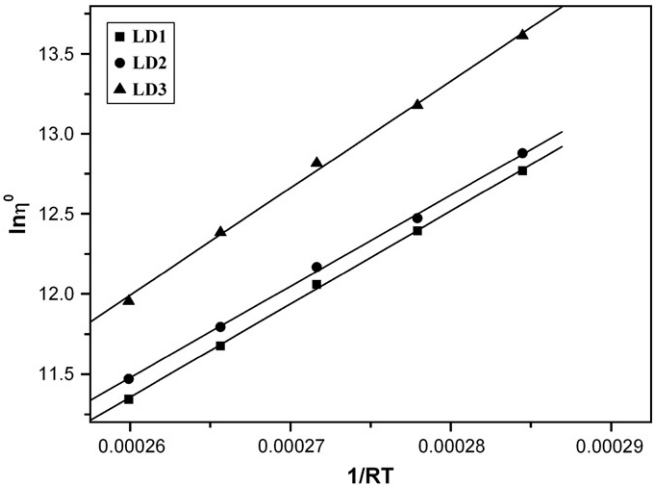

Fig. 9. Linear fitting of Guzman–Andrade equation. Flow activation energy of the three LDPE samples is 58 kJ, 57 kJ and 67 kJ for LD1, LD2 and LD3, respectively.

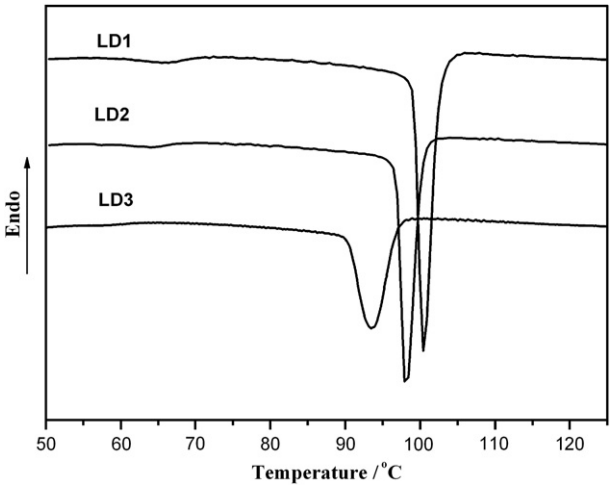

Fig. 10. Crystallization exotherms of LDPE resins.

It was observed in the present experiment that sample LD3 shows higher zero-shear viscosity, higher melt elasticity and flow activation energy (Fig. 9). Based on the above observations, it can be confidently concluded that sample LD3 has higher concentration of long-chain branches. It should be pointed out here that rheological relevant branch lengths are different from those detected by NMR method, because NMR counts all side chain branches although some of them may be of no rheological importance or contribute insignificantly to the reducing of radii of gyration, but rheological method only counts those long enough to entangle in polymer melt, that is at least 180 carbon atoms for PE [28].

Before concluding, it is worth mentioning the LDPE resins' crystallization behavior, which is determined exclusively by the molecular architecture. The magnitude of crystallinity is greatly affected by the overall side chain branching. The possible reason is that as the degree of side chain branching increases, the irregular chain can prevent these segments from folding sequentially into crystalline lattice, correspondingly lowering the crystallinity. Furthermore, it is postulated that the higher molecular weight component in polymer is difficult to crystallize, however, it can act as a nucleation agent which can promote more rapid nucleation, but the crystallization rate will not increase accordingly as it is inhibited by the growth rate of crystallization, due to the higher melt elasticity. When examining the DSC crystallization exotherms (Fig. 10), it can be found that sample LD3 which has distinctly larger portion of higher molecular weight component shows apparently broader exothermic peak, indicating a slower crystallization rate than the other two samples. Mandelkern et al. studied the mixtures of linear polyethylene resins by light scattering and showed that adding even small amount of high M_w fraction into a lower M_w fraction led to a deterioration of spherulitic morphology [29]. The above argues strongly suggest that the high molecular weight tail displayed in sample LD3 is crucial in impeding the development of spherulites or other superstructures and as a result leading to a much smaller stacked lamellar structure. However, the haze is not lowered necessarily as expected, due to the fact that the haze of the films studied depends primarily on the extrusion roughness rather than the crystal texture. The high molecular weight tail in sample LD3 promotes longer relaxation time and higher irreversible shear or elasticity which is primarily responsible for the vast majority of the surface irregularities and hence higher haze.

4. Conclusions

By carrying out a combinatorial investigation of DSC, WAXD, SEM, optical haze, GPC, NMR, as well as rheological measurements in three LDPE blown films with different optical properties, a systematic relationship among the molecular architecture, rheological property and relaxation behavior, crystal structure and surface irregularity and the ultimate optical haze has been established. The surface irregularity rather than the bulk inhomogeneity of LDPE blown films is mainly responsible for the total haze. The surface irregularity depends primarily on the rheological property of the melt rather than the surface crystal structures. The localized melt fracture and extrusion instability which cannot be alleviated by the following extension smoothing effect due to its slow relaxation and high melt elasticity are primarily responsible for surface irregularity. The very high molecular weight, broad molecular weight distribution and long-chain branch density play the key roles in causing surface roughness and consequently enhancing surface and total haze for LDPE blown films.

Acknowledgement

This work was supported by the NSFC-SinoPec Joint Project.

References

[1] Willmouth FM. Optical properties of polymers. London: Elsevier; 1986.
[2] Johnson MB, Wilkes GL, Sukhdia AM, Rohlfing DC. J Appl Polym Sci 2000;77:2845.
[3] Clegg PL, Huck ND. Plastics 1961;114.

[4] Huck ND, Clegg PL. SPE Trans 1961;121.
[5] Clampitt BH, German DE, Hanson HD. Anal Chem 1969;41:1306.
[6] Stehling FC, Speed CS, Westerman L. Macromolecules 1981;14:698.
[7] White JL, Matsukura Y, Kang HJ, Yamane H. Int Polym Proc 1987;1:83.
[8] Pucci MS, Shroff RN. Polym Eng Sci 1986;26:569.
[9] Kojima M, Magill JH, Lin JS, Magonov SN. Chem Mater 1997;9:1145.
[10] Samuels RJ. J Polym Sci Polym Phys Ed Part A-2 1969;7:1197.
[11] Haudin JM, Piana A, Monasse B, Monge G, Gourdon B. Ann Chim Sci Mater 1999;24:555.
[12] Hashimoto T, Todo A, Murakami Y, Kawai H. J Polym Sci Polym Phys Ed 1977;15:501.
[13] Pinto G, Larena A. Polym Eng Sci 1993;33:742.
[14] Stover JC. Optical scattering measurements and analysis. 2nd ed. Bellingham, Washington: SPIE Optical Engineering Press; 1995.
[15] Wang L, Kamal MR, Rey AD. Polym Eng Sci 2001;41:358.
[16] Neves CJ, Monteiro E, Habert AC. J Appl Polym Sci 1993;50:817.
[17] Wunderlich B. Thermal characterization of polymeric materials. 2nd ed., vol. 1. New York: Academic Press; 1997.
[18] Kuwabara K, Kaji H, Horii F, Bassett DC, Olley RH. Macromolecules 1997;30:7516.
[19] Zhu SN. Macromolecular chain structure. Beijing: Science Press; 1996.
[20] Magill JH, Peddada SV. J Polym Sci Polym Phys Ed 1979;17:947.
[21] Sukhadia AM, Rohlfing DC, Wilkes GL, Johnson MB. J SPE ANTEC 2001;6–10.
[22] Rokudi M. J Appl Polym Sci 1979;23:463.
[23] Fujiki T. J Appl Polym Sci 1971;15:47.
[24] Rudin A, Schreiber HP. Polym Eng Sci 1983;23:422.
[25] Keating M, Lee IH, Wong CS. Thermochim Acta 1996;284:47.
[26] Peeters M, Goderis B, Vonk C, Reynaers H, Mathot V. J Polym Sci Part B Polym Phys 1997;35:2689.
[27] Wood-Adams PM, Costeux S. Macromolecules 2001;34:6281.
[28] Bailly C, Stephenne V, Daoust D, Godard P, Ruymbeke EV, Keunings R. Polym Prepr (Am Chem Soc Div Polym Chem) 2003;44:35.
[29] Mandelkern L, Go S, Peiffer D, Stein RS. J Polym Sci Polym Phys Ed 1977;15:1189.